Dynamics of a tracer granular particle as a nonequilibrium Markov process

Andrea Puglisi,[1] Paolo Visco,[1,2] Emmanuel Trizac,[2] and Frédéric van Wijland[1,3]
[1]*Laboratoire de Physique Théorique (CNRS UMR8627), Bâtiment 210, Université Paris-Sud, 91405 Orsay Cedex, France*
[2]*Laboratoire de Physique Théorique et Modèles Statistiques (CNRS UMR 8626), Bâtiment 100, Université Paris-Sud, 91405 Orsay Cedex, France*
[3]*Laboratoire de Matière et Systèmes Complexes (CNRS UMR 7057), Université Denis Diderot (Paris VII), 2 place Jussieu, 75251 Paris Cedex 05, France*
(Received 19 September 2005; published 2 February 2006)

The dynamics of a tracer particle in a stationary driven granular gas is investigated. We show how to transform the linear Boltzmann equation, describing the dynamics of the tracer into a master equation for a continuous Markov process. The transition rates depend on the stationary velocity distribution of the gas. When the gas has a Gaussian velocity probability distribution function (PDF), the stationary velocity PDF of the tracer is Gaussian with a lower temperature and satisfies detailed balance for any value of the restitution coefficient α. As soon as the velocity PDF of the gas departs from the Gaussian form, detailed balance is violated. This nonequilibrium state can be characterized in terms of a Lebowitz-Spohn action functional $W(\tau)$ defined over trajectories of time duration τ. We discuss the properties of this functional and of a similar functional $\bar{W}(\tau)$, which differs from the first for a term that is nonextensive in time. On the one hand, we show that in numerical experiments (i.e., at finite times τ), the two functionals have different fluctuations and $\bar{W}$ always satisfies an Evans-Searles-like symmetry. On the other hand, we cannot observe the verification of the Lebowitz-Spohn-Gallavotti-Cohen (LS-GC) relation, which is expected for $W(\tau)$ at very large times τ. We give an argument for the possible failure of the LS-GC relation in this situation. We also suggest practical recipes for measuring $W(\tau)$ and $\bar{W}(\tau)$ in experiments.

DOI: 10.1103/PhysRevE.73.021301 PACS number(s): 45.70.−n, 05.20.Dd, 05.40.−a

I. INTRODUCTION

When a collection of macroscopic grains (diameter ranging from 10^{-4} cm up to 10^{-1} cm) is vigorously shaken, under appropriate conditions of packing fraction, amplitude, and frequency of the vibration, a stationary gaseous state, usually referred to as "granular gas," can be obtained [1]. Kinetic energy is dissipated into heat during collisions among grains, and this energetic loss is balanced by the external driving, i.e., the shaking of the container. In recent years, the interest in granular gases has strongly increased: it has been shown that the whole machinery of kinetic theory can be applied to simplified but realistic models, leading to theoretical results in good agreement with experiments [2,3]. At the same time, a growingly rich phenomenology has emerged from the laboratory, showing that a granular gas is a sort of Pandora's box for nonequilibrium statistical mechanics. Just to mention the most famous and well-established aspects of these systems, we recall that a granular gas displays non-Gaussian velocity behavior, the breakdown of energy equipartition and of thermodynamic equilibrium, spontaneous breaking of many symmetries (shear instability, cluster instability, convection instability, etc.), and a general strong tendency to reduce the range of scales available to a hydrodynamic description. Nevertheless, in a carefully controlled environment, one can avoid all spatial effects, obtaining a homogeneous granular gas whose main feature is to be stationary and out of thermodynamic equilibrium, traversed by an energy current that flows from the external driving into an irreversible sink constituted by the inelastic collisions among the grains. In this case, it is straightforward to measure a so-called granular temperature $T_g=\langle|\mathbf{v}|^2/d\rangle$ (where d is the space dimension), which is different, in general, from the temperature T characterizing the external driving. We stress that, in real experiments, it is hard to obtain a stochastic way of pumping energy into a granular gas: the simplest situation is a vertically vibrating mechanism, where density gradients arise. In this paper, our interest goes to models where the action of the external driving is, in fact, that of a homogeneous thermostat. Such a kind of homogeneous heating has already been achieved, experimentally, with a granular monolayer vibrated on a rough plate [4]. Very recently, granular gases have been used to probe the latest theoretical results concerning fluctuations in nonequilibrium systems. In particular, the so-called Gallavotti-Cohen fluctuation relation (GCFR) [5] has been put under scrutiny [6,7]. This relation is a constraint in the probability distribution function (PDF) of the fluctuations of entropy flux in the system, which is rigorously demonstrated under certain hypothesis when the entropy flux is measured by the phase space contraction rate. Of course, an all-purpose definition of "entropy flux" in systems out of equilibrium does not exist. The authors of those recent studies have tried to use the rate of energy injection from the external driving (i.e., the injected power) as an entropy flux. Even if in [6] a verification of the GCFR was claimed, other studies have shown that the situation is more complex and that, in general, the injected power in a granular gas cannot satisfy such a relation [8]. The main difference between a granular gas and the prototypical system that should obey the GCFR is the invariance under microscopic time reversal, which is violated by inelastic collisions.

In this paper, we have tried to follow a simplified line of reasoning, obtaining a recipe to measure a "flux" that is constructed *ad hoc* with the aim of satisfying the GCFR, or at least its Markovian counterpart, which has been put forward by Lebowitz and Spohn [9]. In the following, we will refer to this relation as to the Gallavotti-Cohen-Lebowitz-Spohn (GC-LS) fluctuation relation. Our idea is to bypass the problem of "strong irreversibility" posed by inelastic collisions (i.e., the fact that the probability of observing the time reversibility of an inelastic collision is strictly zero), focusing on the evolution of a tracer particle [10,11]. Indeed, in a dilute gas, a tracer particle performs a continuous Markov process characterized by transition rates, which are always defined (i.e., for any observable transition the time-reversed transition has a nonzero probability). Therefore, the projection of a N-body system onto a one-body system somehow increases its degree of time reversibility.

Our original aim was to find a quantity, for granular gases, which, by construction, verifies the GC-LS fluctuation relation. Besides, the use of a single-particle functional is still interesting because it can easily be reproduced in real experiments. Moreover, the fluctuations of this functional are much stronger than the fluctuations of some other observable that is averaged over a large number of particles, and this is an evident advantage in an experimental verification of a fluctuation relation. Anyway, we will show by numerical simulations that this verification poses unexpected problems, even after having followed carefully the recipe given by Lebowitz and Spohn. Only at very large integration times and for situations very far from equilibrium, the GC-LS fluctuation relation is near to being satisfied. At the same time, an alternative functional can be defined, differing from the first one by an apparently small term. This second functional always satisfies a relation, which we consider the Markovian counterpart of the Evans-Searles (ES) fluctuation relation [12,13]. In summary, our investigation has led to a concrete example, ready to become a real experiment, where the difference between two fluctuation relations, their meaning, and their limits can directly be probed.

The structure of the paper is as follows: in Sec. II, we define our model and its description in terms of a continuous Markov process, i.e., giving the transition rates that enter its master equation. We also show that, whenever the surrounding gas has a non-Gaussian velocity distribution, the tracer particle violates detailed balance and is therefore out of equilibrium. In Sec. III, we define the action functionals that are expected to verify the GC-LS and ES fluctuation relations. In Sec. IV, we discuss the results of numerical simulations, showing a way to optimally measure the transition rates and, finally, discussing the measure of the fluctuations of the action functionals and their verification of the fluctuation relations. We will draw our conclusions in Sec. V. The derivation of the master equation from the linear Boltzmann equation is given in the Appendix.

II. THE MASTER EQUATION

We consider the dynamics of a tracer granular particle in a homogeneous and dilute gas of grains that is driven by an unspecified energy source. The first essential feature of the gas is its spatial and temporal homogeneity. The tracer particle collides, sequentially, with particles of the gas coming from the same "population," independently of the position and time of the collision. The gas is characterized by its velocity probability density function $P(\mathbf{v})$, which, in turn, is determined by the unspecified details of the model, such as the properties of the driving or of the grains. It is well known that the velocity probability density function of a driven granular gas is non-Gaussian: in a homogeneous setup, the slight departure from Gaussianity is well reproduced by a first Sonine correction (which will be made explicit in the following). This is expected theoretically and well verified in experiments [14].

The second essential property required is the diluteness of the gas: it guarantees that the assumption of molecular chaos is valid, which means that the evolution as well as the stationary regime of the velocity probability density function $P_*(\mathbf{v})$ of the tracer is governed by a linear Boltzmann equation. In this section, we give expressions for the tracer transition rates in generic dimension d and for a generic interparticle (short-range) potential. This potential is parametrized by a parameter γ, which is the exponent of the term $|(\mathbf{v}-\mathbf{V})\cdot\hat{\boldsymbol{\omega}}|^{\gamma}$, representing the collision kernel in the linear Boltzmann equation ($\mathbf{v}$ and $\mathbf{V}$ are the colliding velocities while $\hat{\boldsymbol{\omega}}$ is the unitary vector joining the particles). For example, a value of $\gamma=1$ corresponds to the hard sphere potential (which will be studied in the rest of the paper, without losing generality in the results), a value of $\gamma=0$ corresponds to the Maxwell Molecules case, and a value of $\gamma=2$ to the so-called very hard particles.

The inelastic collisions with the gas particles, which solely determine the instantaneous changes of the velocity of the tracer, are described by the simplest and most used inelastic collision rule:

$$\mathbf{v}' = \mathbf{v} - m\frac{1+\alpha}{m+M}[(\mathbf{v}-\mathbf{V})\cdot\hat{\boldsymbol{\omega}}]\hat{\boldsymbol{\omega}}, \tag{1}$$

where $\mathbf{v}$ and $\mathbf{v}'$ are the velocities of the tracer before and after the collision, respectively; $\mathbf{V}$ is the velocity of the gas particle; M and m are the masses of the tracer and of the gas particle, respectively; while $\hat{\boldsymbol{\omega}}$ is the unitary vector joining the centers of the two particles. The restitution coefficient $\alpha\in[0,1]$ parametrizes the inelasticity of the collision (it is 1 when the collision is elastic). In the following, we will assume $m=M$, but this will not change the generality of our results, in view of the following relation:

$$m\frac{1+\alpha}{m+M} \equiv \frac{1+\alpha'}{2}, \quad \text{with} \quad \alpha' = \frac{m-M+2m\alpha}{m+M}. \tag{2}$$

The γ-Boltzmann equation for the tracer, in generic dimension d, reads

$$\frac{\mathrm{d}P_*(\mathbf{v},t)}{\mathrm{d}t} = \frac{v_0^{1-\gamma}}{l_0}\int \mathrm{d}\mathbf{v}_1 \int \mathrm{d}\mathbf{v}_2 \int' \mathrm{d}\hat{\omega}|(\mathbf{v}_1-\mathbf{v}_2)\cdot\hat{\omega}|^{\gamma} P_*(\mathbf{v}_1) \times P(\mathbf{v}_2)\left\{\delta\left(\mathbf{v}-\mathbf{v}_1+\frac{1+\alpha}{2}[(\mathbf{v}_1-\mathbf{v}_2)\cdot\hat{\omega}]\hat{\omega}\right) - \delta(\mathbf{v}-\mathbf{v}_1)\right\}, \tag{3}$$

where the primed integral denotes that the integration is performed on all angles that satisfy $(\mathbf{v}_1-\mathbf{v}_2)\cdot\hat{\boldsymbol{\omega}}>0$. The mean free path l_0 appears in front of the collision integrals. In the $\gamma\neq 1$ cases, to respect dimensionality, a factor $v_0^{1-\gamma}$ is also present, where v_0 is the gas thermal velocity. In the following (when not stated differently), we will put $l_0=1$ and $v_0=1$, which can be always obtained by a rescaling of time. Note that, as expressed before, the velocity of the tracer is affected only by collisions with the gas particles, since it is not coupled to the external thermostat.

From the analysis of Eq. (3) given in Appendix, we find that the evolution of the velocity probability density function of the tracer is governed by the following Master equation:

$$\frac{dP_*(\mathbf{v},t)}{dt}=\int d\mathbf{v}_1 P_*(\mathbf{v}_1)K(\mathbf{v}_1,\mathbf{v})-\int d\mathbf{v}_1 P_*(\mathbf{v})K(\mathbf{v},\mathbf{v}_1), \tag{4}$$

where $P_*(\mathbf{v})$ is the velocity PDF of the test particle. The transition rate $K(\mathbf{v},\mathbf{v}')$ of jumping from $\mathbf{v}$ to $\mathbf{v}'$ is given by the following formula:

$$K(\mathbf{v},\mathbf{v}')=\left(\frac{2}{1+\alpha}\right)^{\gamma+1}\frac{v_0^{1-\gamma}}{l_0}|\Delta\mathbf{v}|^{\gamma-d+1}\int d\mathbf{v}_{2\tau}P[\mathbf{v}_2(\mathbf{v},\mathbf{v}',\mathbf{v}_{2\tau})], \tag{5}$$

where $\Delta\mathbf{v}=\mathbf{v}'-\mathbf{v}$ denotes the change of velocity of the test particle after a collision. The vectorial function $\mathbf{v}_2$ is defined as

$$\mathbf{v}_2(\mathbf{v},\mathbf{v}',\mathbf{v}_{2\tau})=v_{2\sigma}(\mathbf{v},\mathbf{v}')\hat{\boldsymbol{\sigma}}(\mathbf{v},\mathbf{v}')+\mathbf{v}_{2\tau}, \tag{6}$$

where $\hat{\boldsymbol{\sigma}}(\mathbf{v},\mathbf{v}')$ is the unitary vector parallel to $\Delta\mathbf{v}$, while $\mathbf{v}_{2\tau}$ is entirely contained in the $(d-1)$-dimensional space perpendicular to $\Delta\mathbf{v}$ (i.e., $\mathbf{v}_{2\tau}\cdot\Delta\mathbf{v}=0$). This implies that the integral in expression (5) is $(d-1)$-dimensional. Finally, to fully determine the transition rate (5), the expression of $v_{2\sigma}$ is needed

$$v_{2\sigma}(\mathbf{v},\mathbf{v}')=\frac{2}{1+\alpha}|\Delta\mathbf{v}|+\mathbf{v}\cdot\hat{\boldsymbol{\sigma}}. \tag{7}$$

Note that Eq. (4) is a master equation for the evolution of a probability density function. We simplify the terminology, using the name "transition rate" for the function $K(\mathbf{v},\mathbf{v}')$, which actually is a "transition-rate density." This density has its natural definition in the following limit:

$$K(\mathbf{v},\mathbf{v}')=\lim_{|d\mathbf{v}'|\to 0}\frac{\mathcal{K}(\mathbf{v}\to\mathbf{u}\in\mathcal{B}_{d\mathbf{v}'}(\mathbf{v}'))}{|d\mathbf{v}'|}, \tag{8}$$

where $\mathcal{K}(\mathbf{v}\to\mathbf{u}\in\mathcal{B}_{d\mathbf{v}'}(\mathbf{v}'))$ is the probability (per unit time) that the tracer, after a collision, has a velocity $\mathbf{u}$ contained in a sphere $\mathcal{B}_{d\mathbf{v}'}(\mathbf{v}')$ of radius $d\mathbf{v}'$ centered in the vector $\mathbf{v}'$, having a velocity $\mathbf{v}$ before the collision.

A. Examples: Gaussian and first Sonine correction

If $P(\mathbf{v})=[1/(2\pi T)^{d/2}]\exp[-(v^2/2T)]$, it then immediately follows that the transition rate $K(\mathbf{v},\mathbf{v}')$ reads

$$K(\mathbf{v},\mathbf{v}')=\left(\frac{2}{1+\alpha}\right)^{\gamma+1}\frac{v_0^{1-\gamma}}{l_0}|\Delta v|^{\gamma-d+1}\frac{1}{\sqrt{2\pi T}}e^{-(v_{2\sigma}^2/2T)}. \tag{9}$$

In kinetic theory, one of the most used corrections to the Gaussian is the first nonzero Sonine polynomial approximation [14,15]. This means assuming that $P(\mathbf{v})=[1/(2\pi T)^{d/2}]\exp[-(v^2/2T)][1+a_2S_2^d(v^2/2T)]$ with $S_2^d(x)=x^2/2-(d+2)x/2+d(d+2)/8$. The calculation of the integral needed to have an explicit expression of the transition rate is straightforward

$$\int d\mathbf{v}_{2\tau}P(\mathbf{v}_2)=\frac{e^{-(v_{2\sigma}^2/2T)}}{\sqrt{2\pi T}}[1+a_2S_2^{d=1}(v_{2\sigma}^2/2T)]. \tag{10}$$

This leads to

$$K(\mathbf{v},\mathbf{v}')=\left(\frac{2}{1+\alpha}\right)^{\gamma+1}\frac{v_0^{1-\gamma}}{l_0}|\Delta v|^{\gamma-d+1}\frac{1}{\sqrt{2\pi T}}\times e^{-(v_{2\sigma}^2/2T)}\left[1+a_2S_2^{d=1}\left(\frac{v_{2\sigma}^2}{2T}\right)\right]. \tag{11}$$

B. Detailed balance

Here, we obtain a simple expression for the ratio between $K(\mathbf{v},\mathbf{v}')$ and $K(\mathbf{v}',\mathbf{v})$. When exchanging $\mathbf{v}$ with $\mathbf{v}'$, the unitary vector $\hat{\boldsymbol{\sigma}}$ changes sign. Furthermore, one has that $v_{2\sigma}(\mathbf{v},\mathbf{v}')\neq v_{2\sigma}(\mathbf{v}',\mathbf{v})$. Finally, it must be recognized that

$$\frac{K(\mathbf{v},\mathbf{v}')d\mathbf{v}'}{K(\mathbf{v}',\mathbf{v})d\mathbf{v}}=\frac{K(\mathbf{v},\mathbf{v}')}{K(\mathbf{v}',\mathbf{v})}. \tag{12}$$

This equivalence is naturally achieved by considering the definition (8) and taking uniformly the two limits $|d\mathbf{v}|\to 0$ and $|d\mathbf{v}'|\to 0$. From all these considerations and from Eq. (5), one obtains immediately

$$\frac{K(\mathbf{v},\mathbf{v}')}{K(\mathbf{v}',\mathbf{v})}=\frac{\int d\mathbf{v}_{2\tau}P[\mathbf{v}_2(\mathbf{v},\mathbf{v}')]}{\int d\mathbf{v}_{2\tau}P[\mathbf{v}_2(\mathbf{v}',\mathbf{v})]}\equiv\frac{P[v_{2\sigma}(\mathbf{v},\mathbf{v}')]}{P[v_{2\sigma}(\mathbf{v}',\mathbf{v})]}. \tag{13}$$

We note that this ratio depends only on the choice of the PDF of the gas, P, and not on the other parameters (such as γ or α). However in realistic situations (experiments or molecular-dynamics simulations) P is not a free parameter but is determined by the choice of the setup (e.g., external driving, material details, geometry of the container, etc.).

Introducing the shorthand notation $v_{2\sigma}=v_{2\sigma}(\mathbf{v},\mathbf{v}')$, $v'_{2\sigma}=v_{2\sigma}(\mathbf{v}',\mathbf{v})$, and $v_\sigma^{(\prime)}=\mathbf{v}^{(\prime)}\cdot\hat{\boldsymbol{\sigma}}$, we also note that

$$(v'_{2\sigma})^2=v_{2\sigma}^2+(v_\sigma+v'_\sigma)^2-2v_{2\sigma}(v_\sigma+v'_\sigma), \tag{14}$$

from which it follows that

$$\Delta_2 = (v_{2\sigma})^2 - (v'_{2\sigma})^2 = -\Delta - 2\frac{1-\alpha}{1+\alpha}\Delta = -\frac{3-\alpha}{1+\alpha}\Delta, \quad (15)$$

where $\Delta = v_\sigma^2 - (v'_\sigma)^2 \equiv |v|^2 - |v'|^2$, i.e., the kinetic energy lost by the test particle during one collision. When $\alpha = 1$, then $\Delta_2 = -\Delta$ (energy conservation). From the above considerations, it follows that

in the Gaussian case, it is found

$$\log \frac{K(\mathbf{v},\mathbf{v}')}{K(\mathbf{v}',\mathbf{v})} = \frac{\Delta}{2T} + 2\frac{1-\alpha}{1+\alpha}\frac{\Delta}{2T} = \frac{3-\alpha}{1+\alpha}\frac{\Delta}{2T}, \quad (16)$$

in the first Sonine correction case, it is found

$$\log \frac{K(\mathbf{v},\mathbf{v}')}{K(\mathbf{v}',\mathbf{v})} = \frac{3-\alpha}{1+\alpha}\frac{\Delta}{2T} + \log \frac{\left\{1 + a_2 S_2^{d=1}\left[\frac{\left(\frac{2}{1+\alpha}(v'_\sigma - v_\sigma) + v_\sigma\right)^2}{2T}\right]\right\}}{\left\{1 + a_2 S_2^{d=1}\left[\frac{\left(\frac{2}{1+\alpha}(v_\sigma - v'_\sigma) + v'_\sigma\right)^2}{2T}\right]\right\}}. \quad (17)$$

In the case where $P(v)$ is a Gaussian with temperature T, it is immediate to observe that

$$P_*(\mathbf{v})K(\mathbf{v},\mathbf{v}') = P_*(\mathbf{v}')K(\mathbf{v}',\mathbf{v}) \quad (18)$$

if P_* is equal to a Gaussian with temperature $T'/T = (\alpha+1)/(3-\alpha) \leqslant 1$. This means that there is a Gaussian stationary solution of Eq. (4) (in the Gaussian-bulk case), which satisfies detailed balance. The fact that such a Gaussian with a different temperature T' is an exact stationary solution was known from Ref. [10]. It thus turns out that detailed balance is satisfied, even out of thermal equilibrium. Of course, this is an artifact of such a model: it is highly unrealistic that a granular gas yields a Gaussian velocity PDF. As soon as the gas velocity PDF $P(v)$ ceases to be Gaussian, detailed balance is violated (i.e., the stationary process performed by the tracer particle is no more in equilibrium within the thermostatting gas). We will see in Sec. III how to characterize this departure from equilibrium.

C. Collision rates

The velocity dependent collision rate is defined as

$$r(\mathbf{v}) = \int d\mathbf{v}' K(\mathbf{v},\mathbf{v}') \equiv \frac{1}{l_0}\int d\mathbf{v}' d\hat{\boldsymbol{\sigma}} \Theta[(\mathbf{v}-\mathbf{v}')\cdot\hat{\boldsymbol{\sigma}}] \times (\mathbf{v}-\mathbf{v}')\cdot\hat{\boldsymbol{\sigma}} P(\mathbf{v}'), \quad (19)$$

where the last passage is true for hard spheres. In the following, for simplicity and for direct comparison to numerical results, we will consider only the model of a two-dimensional hard sphere gas. In this particular case, the collision rate reads for a Gaussian bulk,

$$r(v) = \frac{\sqrt{\pi}}{l_0\sqrt{2T}} e^{-(v^2/4T)}\left[(2T+v^2) I_0\left(\frac{v^2}{4T}\right) + v^2 I_1\left(\frac{v^2}{4T}\right)\right], \quad (20)$$

where $I_n(x)$ is the nth modified Bessel function of the first kind. Note that from Eq. (20), one obtains the total collision frequency

$$\omega_c = \frac{1}{T'}\int dv v e^{-(v^2/2T')} r(v) = \frac{\sqrt{2\pi(T+T')}}{l_0} = \frac{2}{l_0}\sqrt{\frac{2\pi}{3-\alpha}T}, \quad (21)$$

which, using $l_0 = 1/n\sigma^2$ for the mean free path gives $\omega_c = 2\sqrt{\pi T} n\sigma^2$ in the case $\alpha = 1$ (i.e., the known result from kinetic theory for the elastic hard disks). Finally, note that $r(v)$ for the Gaussian case *does not depend* on the restitution coefficient (while the transition rates and the total collision frequency do).

For a bulk with a Gaussian distribution plus the first Sonine approximation,

$$r(\mathbf{v}) = \frac{\sqrt{\pi}}{l_0 8\sqrt{2}T^{5/2}} e^{-(v^2/4T)}(8(1+a_2)T^2 - 8a_2 T v^2 + a_2 v^4) \times \left[(2T+v^2) I_0\left(\frac{v^2}{4T}\right) + v^2 I_1\left(\frac{v^2}{4T}\right)\right]. \quad (22)$$

In this case, the expression for ω_c is more involved.

III. NON-EQUILIBRIUM CHARACTERIZATION

From Sec. II, we have learned that the dynamics of the velocity of a tracer particle immersed in a granular gas is equivalent to a Markov process with well-defined transition rates. This means that the velocity of the tracer particle stays in a state $\mathbf{v}$ for a random time $t \geqslant 0$ distributed with the law $r(v)e^{-r(v)t}dt$ and then makes a transition to a new value $\mathbf{v}'$ with a probability $r(v)^{-1}K(\mathbf{v},\mathbf{v}')$. At this point, it is interesting to ask about some characterizations of the nonequilibrium dynamics, i.e., of the violation of detailed balance, which we know to happen whenever the surrounding granular gas has a non-Gaussian distribution of velocity.

To this extent, we define two different action functionals, following [9]:

$$W(t) = \sum_{i=1}^{n(t)} \log \frac{K(\mathbf{v}_i \to \mathbf{v}'_i)}{K(\mathbf{v}'_i \to \mathbf{v}_i)} \quad (23a)$$

$$\bar{W}(t) = \log \frac{P_*(\mathbf{v}_1)}{P_*(\mathbf{v}'_{n(t)})} + \sum_{i=1}^{n(t)} \log \frac{K(\mathbf{v}_i \to \mathbf{v}'_i)}{K(\mathbf{v}'_i \to \mathbf{v}_i)} \equiv \log \frac{\mathcal{P}(\mathbf{v}_1 \to \mathbf{v}_2 \to \cdots \to \mathbf{v}_{n(t)})}{\mathcal{P}(\mathbf{v}_{n(t)} \to \mathbf{v}_{n(t)-1} \to \cdots \to \mathbf{v}_1)}, \quad (23b)$$

where i is the index of collision suffered by the tagged particle, $\mathbf{v}_i$ is the velocity of the particle before the ith collision, $\mathbf{v}'_i$ is its post-collisional velocity, $n(t)$ is the total number of collisions in the trajectory from time 0 up to time t, and K is

the transition rate of the jump due to the collision. Finally, we have used the notation $\mathcal{P}(\mathbf{v}_1 \to \mathbf{v}_2 \to \ldots \to \mathbf{v}_n)$ to identify the probability of observing the trajectory $\mathbf{v}_1 \to \mathbf{v}_2 \to \ldots \to \mathbf{v}_n$. The quantities $W(t)$ and $\bar{W}(t)$ are different for each different trajectory (i.e., sequence of jumps) of the tagged particle. The first term $\log P_*(\mathbf{v}_1)/P_*(\mathbf{v}'_{n(t)})$ in the definition of $\bar{W}(t)$ [Eq. (23b)] will be called in the following "boundary term" to stress its nonextensivity in time.

The two above functionals have the following properties:

(i) $W(t) \equiv 0$ if there is exact symmetry, i.e., if $K(\mathbf{v}_i \to \mathbf{v}_{i+1}) = K(\mathbf{v}_{i+1} \to \mathbf{v}_i)$ (e.g., in the microcanonical ensemble);

(ii) $\bar{W}(t) \equiv 0$ if there is detailed balance (e.g., any equilibrium ensemble);

(iii) we expect that, for t large enough, for almost all the trajectories $\lim_{s\to\infty} W(s)/s = \lim_{s\to\infty} \bar{W}(s)/s = \langle W(t)/t \rangle = \langle \bar{W}(t)/t \rangle$; here (since the system under investigation is ergodic and stationary) the meaning of the angular brackets is intuitively an average over many independent segments of a single, very long trajectory;

(iv) for large enough t, at equilibrium $\langle W(t) \rangle = \langle \bar{W}(t) \rangle = 0$ and also out of equilibrium (i.e., if detailed balance is not satisfied), those two averages are positive; we use those equivalent averages, at large t, to characterize the distance from equilibrium of the stationary system.

(v) If $S(t) = -\int \mathrm{d}v P_*(v,t) \log P_*(v,t)$ is the entropy associated to the PDF of the velocity of the tagged particle $P_*(v,t)$ at time t (e.g., $-H$ where H is the Boltzmann-H function), then

$$\frac{\mathrm{d}}{\mathrm{d}t} S(t) = R(t) - A(t), \tag{24}$$

where $R(t)$ is always non-negative, $A(t)$ is linear with respect to P_*, and, finally, $\langle W(t) \rangle \equiv \int_0^t \mathrm{d}t' A(t')$. This leads one to consider the $W(t)$ equivalent to the contribution of a single trajectory to the total entropy flux. In a stationary state, $A(t) = R(t)$ and, therefore, the flux is equivalent to the production; this property has been recognized in Ref. [9].

(vi) FR_W (Lebowitz-Spohn-Gallavotti-Cohen fluctuation relation): $\pi(w) - \pi(-w) = w$, where $\pi(w) = \lim_{t\to\infty} (1/t) \log f^t_W(tw)$ and $f^t_W(x)$ is the probability density function of finding $W(t) = x$ at time t; at equilibrium, the FR_W has no content; note that, in principle, $\pi'(w,t) = (1/t) \log f^t_W(tw) \neq \pi(w)$ at any finite time; a generic derivation of this property has been obtained in [9], while a rigorous proof with more restrictive hypothesis is given in [16]; the discussion for the case of a Langevin equation is presented in [17].

(vii) $FR_{\bar{W}}$ (Evans-Searles fluctuation relation): $\bar{\pi}(w,t) - \bar{\pi}(-w,t) = w$ where $\bar{\pi}(w,t) = (1/t) \log f(t/\bar{W})(tw)$ and $(ft/\bar{W})(x)$ is the probability density function of finding $\bar{W}(t) = x$ at time t; at equilibrium the $FR_{\bar{W}}$ has no content;

On the one side we have called FR_W a Lebowitz-Spohn-Gallavotti-Cohen fluctuation relation, following Ref. [9], where the analogy with the original Gallavotti-Cohen fluctuation relation has been stated explicitly. On the other side, we have called the $FR_{\bar{W}}$ a "Evans-Searles" fluctuation relation, inspired by the following analogy. The original Gallavotti-Cohen fluctuation theorem concerns the fluctuation of a functional $\Omega(t)$, which is the time-averaged phase-space contraction rate, i.e.,

$$t\Omega(t) \equiv \int_0^t \Lambda(\Gamma(s)) \mathrm{d}s, \tag{25}$$

where $\Lambda(\Gamma(s))$ is the phase-space contraction rate at the point $\Gamma(s)$ in the phase space visited by the system at time s. On the other side, the original Evans-Searles fluctuation theorem [12,13] concerns the fluctuations of a functional $\bar{\Omega}(t)$ (often called "dissipation function") defined as

$$\begin{aligned} t\bar{\Omega}(t) &\equiv \log\left(\frac{f(\Gamma(0))}{f(\Gamma(t))}\right) - \int_0^t \Lambda(\Gamma(s)) \mathrm{d}s \\ &\equiv \log \frac{p(\delta V_\Gamma(\Gamma(0)))}{p(\delta V_\Gamma(I_T \Gamma(t)))}, \end{aligned} \tag{26}$$

where $f(\Gamma)$ is the phase-space density function at time 0, $p(\delta V_\Gamma(\Gamma))$ is the probability of observing at time 0 an infinitesimal phase space volume of size δV_Γ around the point Γ, and I_T is the time-reversal operator, which typically leaves the position unaltered and changes the sign of the velocities. The last equality in Eq. (26) follows from the Liouville equation written in Lagrangian form: $\mathrm{d}f(\Gamma,t)/\mathrm{d}t = -\Lambda(\Gamma) f(\Gamma,t)$ (details on its derivation can be found in Ref. [13]). The ratio of probabilities appearing at the end of the right-hand side of (26) can be thought of as the deterministic equivalent of the ratio of probabilities appearing at the end of the right-hand side of definition (23b). The term $\log f(\Gamma(0))/f(\Gamma(t))$ is instead analogous to the term $\log P_*(\mathbf{v}_1)/P_*(\mathbf{v}'_{n(t)})$, since the system can be prepared at time 0 in such a way that its phase-space density function f is arbitrarily near its stationary invariant measure. The analogy between those two terms and, therefore, between the two pairs of functionals $\Omega, \bar{\Omega}$ and $W, \bar{W}$ cannot be derived mathematically rigorously, at the moment, but formally at least, it looks rather convincing. Note also that the difference between the two functionals of each couple vanishes when the invariant phase-space distribution function becomes constant, e.g., in the microcanonical ensemble.

As a final remark of this section, consider the more general case where the tracer particle also feels the external driving; this means that other transitions are possible. The simplest case corresponds to an external driving modeled as a thermostat that acts on the grains in the form of independent random kicks [14]. It is straightforward to recognize that the transition rates competing with the velocity changes due to these kicks are symmetric and therefore do not contribute to the action functionals in Eq. (23). On the other hand, when one wants to include the effect of walls (both still or vibrating), new transition rates should be taken into account. A collision with a wall can be modeled as a collision with a flat body with infinite mass, so that

$$v'_\sigma = -\alpha_w v_\sigma + (1+\alpha_w)v_w(t), \tag{27}$$

where σ is the direction perpendicular to the wall and $v_w(t)$ is the wall velocity in that direction at the time t of the collision, while α_w is the restitution coefficient, which describes the energy dissipation during such a collision. If the wall is still ($v_w=0$) and $\alpha_w<1$, then the transition is nonreversible and this results in a divergent contribution to the action functionals. If the wall is still but elastic, then again the transition rates are symmetric and do not contribute to the action functionals. Finally, if the wall is vibrating, the transition rates will depend on the probability $P_w(v_w=x)$ of finding the vibrating wall at a certain velocity x.

IV. NUMERICAL SIMULATIONS

A Direct Simulation Monte Carlo (DSMC) [18] is devised to simulate in dimension $d=2$ the dynamics of a tracer particle undergoing inelastic collisions with a gas of particles in a stationary state with a given velocity PDF $P(\mathbf{v})$. The simulated model contains three parameters: the restitution coefficient α, the temperature of the gas T (which we take as unity), and the coefficient of the first Sonine correction, which parametrizes the velocity PDF of the gas, a_2. The tracer particle has a "temperature" $T_*<T$ and a velocity PDF that is observed to be well described again by a first Sonine correction to a Gaussian, parametrized by a coefficient a_2^*. We also use $l_0=1$. This means that the elastic mean free time is $\tau_c^{el}=1/2\sqrt{\pi}$ (it is larger in inelastic cases). Note that in our numerical work we have chosen to explore the restricted range $\alpha\in[0,1]$. The use of an effective restitution coefficient α', taking values outside of this range ($\alpha'\in[-1,3]$) is justified when $M/m\neq 1$ by the relation (2). We have preferred to avoid the complication of different masses, a case that would require a careful study of the stationary velocity pdfs and their departure from the Gaussian.

The quantities $W(\tau)$ and $\bar{W}(\tau)$ are measured along independent (nonoverlapping) segments of time length τ extracted from a unique trajectory.

A. Verification of transition rates formula

In this section, we verify the correctness of formula (9) for the Gaussian bulk and formula (11) for the non-Gaussian (Sonine-corrected) bulk. Since the algorithm used (the DSMC [18]) is known to very well reproduce the molecular chaos assumption, which is the unique hypothesis used to obtain those formula, we consider this verification a mere check of the consistency of algorithms and calculations. On the other side, while performing this verification, we have devised a way of optimizing the measurement of the transition rates, which can be adopted in experiments.

The brute-force method of measuring K in an experiment or a simulation is to observe subsequent collisions for a long time t and cumulate them in a four-dimensional ($2d$-dimensional) matrix DY_t: this means that $DY_t(v_x,v_y,v'_x,v'_y)$ contains the number of observed collisions such that the precollisional and postcollisional velocities are contained in a cubic region centered in (v_x,v_y,v'_x,v'_y) and of volume $dv_x\times dv_y\times dv'_x\times dv'_y$ finite but small. At the same time, it is necessary to measure $P_*(v_x,v_y)dv_xdv_y$ for the tagged particle. These quantities are related by the following formula:

$$DY_t(v_x,v_y,v'_x,v'_y) = tP_*(v_x,v_y)K(\mathbf{v},\mathbf{v}')dv_xdv_ydv'_xdv'_y, \tag{28}$$

which can be immediately inverted to obtain $K(\mathbf{v},\mathbf{v}')$. Anyway, this recipe may require a very large statistics, because of the high dimensionality of the histogram DY_t.

Then we note that K is a function of only $v_\sigma, v_{\sigma'}$. It becomes tempting, therefore, to reduce the number of variables from $2d$ to 2 in order to optimize the procedure. A histogram $D\tilde{Y}_t$ of dimensionality 2 (in any dimension) can be obtained, so that each element $D\tilde{Y}_t(u_\sigma,u'_\sigma)$ contains the number of observed collisions such that the projection along the direction $\hat{\boldsymbol{\sigma}}$ of the precollisional velocity is u_σ and that of the postcollisional velocity is u'_σ. We note that

$$\begin{aligned}
D\tilde{Y}_t(u_\sigma,u'_\sigma) &= du_\sigma du'_\sigma \int DY_t(v_x,v_y,v'_x,v'_y)\,\delta(u_\sigma \\
&\quad - \mathbf{v}\cdot\hat{\boldsymbol{\sigma}}(\mathbf{v},\mathbf{v}'))\,\delta(u'_\sigma - \mathbf{v}'\cdot\hat{\boldsymbol{\sigma}}(\mathbf{v},\mathbf{v}')) \\
&= du_\sigma du'_\sigma t \int dv_x dv_y dv'_x dv'_y K(\mathbf{v},\mathbf{v}')P_*(\mathbf{v})\,\delta(u_\sigma \\
&\quad - \mathbf{v}\cdot\hat{\boldsymbol{\sigma}}(\mathbf{v},\mathbf{v}'))\,\delta(u'_\sigma - \mathbf{v}'\cdot\hat{\boldsymbol{\sigma}}(\mathbf{v},\mathbf{v}')) \\
&= du_\sigma du'_\sigma t \int dv_x dv_y \int dv'_\sigma dv'_\sigma \mathcal{J}(v_x,v_y,v_\sigma,v'_\sigma) \\
&\quad \times K(\mathbf{v},\mathbf{v}')P_*(\mathbf{v})\,\delta(u_\sigma - v_\sigma)\,\delta(u'_\sigma - v'_\sigma).
\end{aligned} \tag{29}$$

In the last passage, we have done the change of variables (at fixed v_x,v_y) $v'_x,v'_y\to v_\sigma(v_x,v_y),v'_\sigma(v_x,v_y)$. This implies the appearing of the associated Jacobian. Moreover, it happens that $\mathbf{v}\cdot\hat{\boldsymbol{\sigma}}(\mathbf{v},\mathbf{v}')\equiv v_\sigma$ and $\mathbf{v}'\cdot\hat{\boldsymbol{\sigma}}(\mathbf{v},\mathbf{v}')\equiv v'_\sigma$. Postponing the problem of finding the Jacobian $\mathcal{J}$, we can absorb the Dirac δ's, obtaining

$$\begin{aligned}
D\tilde{Y}_t(u_\sigma,u'_\sigma) &= du_\sigma du'_\sigma t\tilde{K}(u_\sigma,u'_\sigma) \\
&\quad \times \int dv_x dv_y \mathcal{J}(v_x,v_y,u_\sigma,u'_\sigma)P_*(\mathbf{v}),
\end{aligned} \tag{30}$$

where $\tilde{K}(u_\sigma,u'_\sigma)$ is just the transition probability K as a function of u_σ,u'_σ (which is its natural representation). The change of variables is given by the following rule:

$$v_\sigma = v_x\frac{v'_x-v_x}{\sqrt{(v'_x-v_x)^2+(v'_y-v_y)^2}} + v_y\frac{v'_y-v_y}{\sqrt{(v'_x-v_x)^2+(v'_y-v_y)^2}} \tag{31a}$$

$$v'_\sigma = v'_x\frac{v'_x-v_x}{\sqrt{(v'_x-v_x)^2+(v'_y-v_y)^2}} + v'_y\frac{v'_y-v_y}{\sqrt{(v'_x-v_x)^2+(v'_y-v_y)^2}}. \tag{31b}$$

After calculations, the Jacobian reads

$$\mathcal{J}=\frac{|v'_\sigma - v_\sigma|}{\sqrt{v_x^2+v_y^2-v_\sigma^2}}\theta(v_x^2+v_y^2-v_\sigma^2). \tag{32}$$

From the expression of the Jacobian, and taking into account the isotropy of $P_*(\mathbf{v})d\mathbf{v}\equiv v\widetilde{P}_*(v)\mathrm{d}v\mathrm{d}\phi$, one gets

$$D\widetilde{Y}_t(u_\sigma,u'_\sigma)=\mathrm{d}u_\sigma \mathrm{d}u'_\sigma t\widetilde{K}(u_\sigma,u'_\sigma)|u'_\sigma-u_\sigma|\mathcal{L}(u_\sigma), \tag{33}$$

where

$$\begin{aligned}\mathcal{L}(u_\sigma)&=\frac{1}{|u'_\sigma-u_\sigma|}\int \mathrm{d}v_x\mathrm{d}v_y\mathcal{J}(v_x,v_y,u_\sigma,u'_\sigma)P_*(\mathbf{v})\\&=\int \mathrm{d}v_x\mathrm{d}v_y\frac{P_*(\mathbf{v})}{\sqrt{v_x^2+v_y^2-u_\sigma^2}}\theta(v_x^2+v_y^2-u_\sigma^2)\\&=2\pi\int_{|u_\sigma|}^{\infty}\mathrm{d}v v\frac{\widetilde{P}_*(v)}{\sqrt{v^2-u_\sigma^2}}=2\pi\int_0^\infty \mathrm{d}z\widetilde{P}_*(\sqrt{z^2+u_\sigma^2}).\end{aligned} \tag{34}$$

As already discussed, the result by Martin and Piasecki [10] explains that when the velocity PDF of the gas is Gaussian, then the tagged particle also has a Gaussian PDF. In particular, if the bulk has a temperature T, the tagged particle has a temperature $T'=(\alpha+1)/(3-\alpha)T$. Then, it is easy to find that

$$K(u_\sigma,u'_\sigma)=\left(\frac{2}{1+\alpha}\right)^2\frac{1}{\sqrt{2\pi T}}e^{-(1/2T)[(2/1+\alpha)(u'_\sigma-u_\sigma)+u_\sigma]^2} \tag{35}$$

and

$$\mathcal{L}(u_\sigma)=\frac{\sqrt{\pi}}{\sqrt{2T'}}e^{-(u_\sigma^2/2T')}, \tag{36}$$

so that the theoretical expectation for the measured array $D\widetilde{Y}_t$ is

$$\begin{aligned}D\widetilde{Y}_t(u_\sigma,u'_\sigma)=\mathrm{d}u_\sigma\mathrm{d}u'_\sigma t\left(\frac{2}{1+\alpha}\right)^2\frac{1}{2\sqrt{TT'}}|u'_\sigma-u_\sigma|\\\times\exp\left[-\frac{1}{2T}\frac{4}{(1+\alpha)^2}\right.\\\left.\times(u_\sigma^2+(u'_\sigma)^2+(\alpha-1)u_\sigma u'_\sigma)\right],\end{aligned} \tag{37}$$

which for the case $\alpha=1$ reads

$$D\widetilde{Y}_t(u_\sigma,u'_\sigma)=\mathrm{d}u_\sigma\mathrm{d}u'_\sigma t\frac{1}{2}\frac{1}{T}|u'_\sigma-u_\sigma|\exp\left\{-\frac{1}{2T}[u_\sigma^2+(u'_\sigma)^2]\right\}. \tag{38}$$

It should be noted that, for any value of α, $D\widetilde{Y}_t$ is symmetric, i.e., $D\widetilde{Y}_t(u_\sigma,u'_\sigma)=D\widetilde{Y}_t(u'_\sigma,u_\sigma)$, and this is the reflection of the fact that, in this Gaussian case, the detailed balance is always satisfied.

In top and middle frames of Fig. 1, the results of DSMC simulations with Gaussian bulk and $\alpha=1$ and $\alpha=0.5$ are shown for some sections of the measured $D\widetilde{Y}_t$, showing the perfect agreement with the theoretical fits.

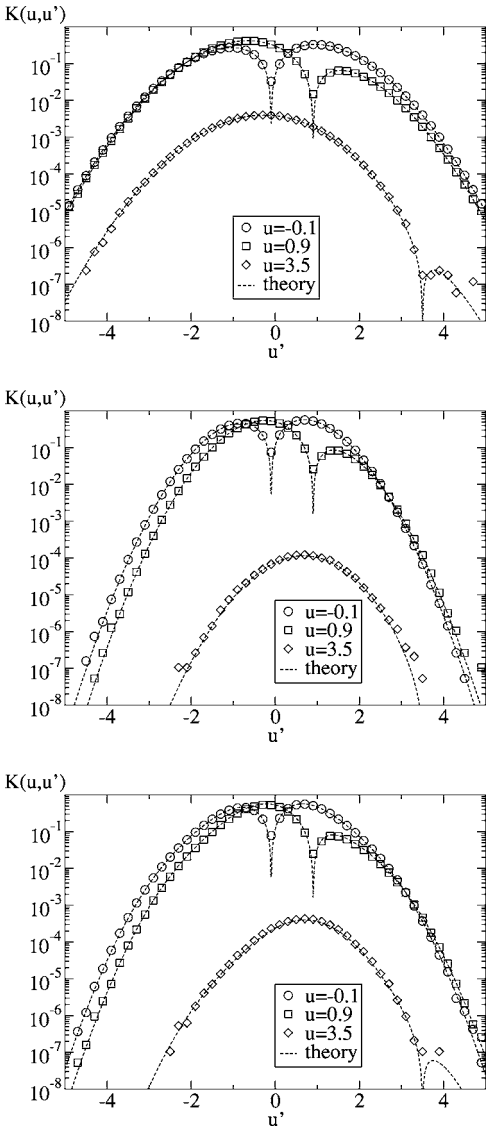

FIG. 1. Measure of transition rates in Monte Carlo simulations. Sections of the function $D\widetilde{Y}(u_\sigma,u'_\sigma)/t\mathrm{d}u_\sigma\mathrm{d}u'_\sigma$ for the values $u_\sigma=-0.1$, $u_\sigma=0.9$, and $u_\sigma=3.5$ for three different cases. Top: the gas has Gaussian velocity PDF with temperature $T=1$ and $\alpha=1$ (thermodynamic equilibrium). Middle: the gas has a Gaussian velocity PDF and $\alpha=0.5$ (detailed balance in absence of thermodynamic equilibrium, $T_*=0.6\equiv T'<T$). Bottom: the gas has a non-Gaussian velocity PDF characterized by a first Sonine correction with $a_2=0.1$ (nonequilibrium stationary state, $T_*=0.62\approx T'<T$ and $a_2^*=0.057\ll a_2$). The dashed lines mark the theoretical expressions given in Eqs. (37)–(39).

Long calculations lead to a similar result for the non-Gaussian case, when the gas has a velocity distribution given by a Gaussian, with temperature T, corrected by the second Sonine polynomial with a coefficient a_2. In this case, an exact theory for the stationary state of the tracer particle does not exist. Nevertheless, numerical simulations show that the velocity distribution of the tracer $P_*(v)$ is well approximated by a Gaussian with temperature T_* corrected by the second

Sonine polynomial with a coefficient a_2^*. In particular, we have evidence that $T_* \approx T' = (\alpha+1)/(3-\alpha)T$ (the Martin-Piasecki temperature, which is exact in the Gaussian case) and $a_2^* < a_2$. For hard spheres, we obtain

$$\frac{D\tilde{Y}_t(u_\sigma, u'_\sigma)}{\mathrm{d}u_\sigma \mathrm{d}u'_\sigma t} = \left(\frac{2}{1+\alpha}\right)^2 \frac{1}{2\sqrt{TT_*}} |u'_\sigma - u_\sigma| \times \exp\left[-\frac{1}{2T}\left(\frac{2}{1+\alpha}(u'_\sigma - u_\sigma) + u_\sigma\right)^2 - \frac{1}{2T_*}u_\sigma^2\right] \times \left[1 + a_2^*\left(\frac{3}{8} - \frac{3}{4}\frac{u_\sigma^2}{T_*} + \frac{u_\sigma^4}{8T_*^2}\right)\right] \times \left\{1 + a_2 S_2^{d=1}\left[\frac{\left(\frac{2}{1+\alpha}(u'_\sigma - u_\sigma) + u_\sigma\right)^2}{2T}\right]\right\}. \tag{39}$$

This formula is very well verified by the transition rates observed in simulations, as shown in the right-most frame of Fig. 1.

B. Fluctuation relations

In this section, we want to show the numerical results obtained measuring $W(\tau)$ and $\bar{W}(\tau)$ in DSMC simulations [18]. In particular, our main aim is to verify the fluctuation relations FR_W and $FR_{\bar{W}}$. Actually, there are three equivalent relations that can be written at finite times τ,

$$as_\tau(W) = \log f^\tau(W) - \log f^\tau(W) = W \tag{40a}$$

$$as_\tau^*(w) = \frac{1}{\tau}[\log f^\tau(\tau w) - \log f^\tau(-\tau w)] = w \tag{40b}$$

$$as_\tau^{**}(q) = \frac{1}{\tau\langle w\rangle}[\log f^\tau(\tau\langle w\rangle q) - \log f^\tau(-\tau\langle w\rangle q)] = q, \tag{40c}$$

where $f^\tau(x)$ is the probability density function of finding one of the two functional after a time τ equal to x (i.e., f_W^τ or $f_{\bar{W}}^\tau$ defined at the beginning of this section), while $\langle w\rangle$ is a long time average of $W(\tau)/\tau$. The verification of the GC-LS fluctuation relation requires the measure of $as_\tau^{**}(q)$ at very large values of τ, for values of q at least of order 1, which corresponds to measure $as_\tau(W)$ for values of W at least of order $\tau\langle w\rangle$ at large values of τ. On the contrary, the verification of the ES fluctuation relation requires Eq. (40a) to be true at all times. We have chosen to display $as_\tau(W)$ versus W as well as $as_\tau(\bar{W})$ versus $\bar{W}$.

To measure the quantity $\bar{W}(\tau)$ on each segment of trajectory, it is assumed that $P_*(\mathbf{V})$ is a Gaussian with a first Sonine correction and the values T_* and a_2^* are measured during the simulation itself and used to compute the "boundary term" appearing in the definition of $\bar{W}$ [Eq. (23b)]. All the results are shown in Fig. 2, for many different choices of the time τ and of the parameters α and a_2. We display in each figure the value of $\langle w\rangle = \lim_{\tau\to\infty} W(\tau)/\tau$. Following the idea that this number is an average entropy production rate, we use it to measure how far from equilibrium our system is. This idea is well supported by the results of our simulations: $\langle w\rangle$ is zero when $a_2 = 0$ and increases as α is decreased and a_2 is increased. We recall that $\lim_{\tau\to\infty} W(\tau)/\tau = \lim_{\tau\to\infty} \bar{W}(\tau)/\tau \equiv \langle w\rangle$, since the difference between the two functionals has zero average at large times τ. We also remark that the distribution of both quantities W and $\bar{W}$ are symmetric at equilibrium (i.e., when $a_2 = 0$).

We first discuss the results concerning the fluctuations of $W(\tau)$, identified in Fig. 2 by square symbols. The PDF of these fluctuations are shown in the insets. They are strongly non-Gaussian, with almost exponential tails, at low values of τ for any choice of the parameters. At large values of τ (many hundreds mean free times), the situation changes with how far from equilibrium the system is. At low values of $\langle w\rangle$, the tails of the distribution are very similar to the ones observed at small times. At higher values of $\langle w\rangle$, the distribution changes with time and tends to become more and more Gaussian. We must put great care into the interpretation of this observation. There is no firm guiding principle able to determine if the time τ and the values of W are large enough to be considered "large deviations." A simplistic approach is the following: every time one observes non-Gaussian tails, then one concludes that these tails are, in fact, large deviations, since "small deviations" should be Gaussian. Anyway this approach is misleading: a sum of random variables can give non-Gaussian tails if the number of summed variables is low and the variables themselves have a non-Gaussian distribution. Therefore, time plays a fundamental role and cannot be disregarded. The observation of non-Gaussian tails alone is useless. We will discuss in Sec. IV C the problems related to the true asymptotics of the PDF of $W(\tau)$. Here we stick to the mere numerical observations: we have not been able to measure negative deviations larger than the ones shown in Fig. 2. Distributions obtained at higher values of τ yielded smaller statistics and very few negative events. Using the distributions at hand, we could not verify the GC-LS fluctuation relation. In the last case, which is very far from equilibrium ($a_2 = 0.3$, $\alpha = 0$), a behavior compatible to the GC-LS fluctuation relation is observed, i.e., $as_\tau(W) \approx W$, but the range of available values of W is much smaller than $\langle W\rangle$. At this stage, and in practice, we consider such results a failure of the GC-LS fluctuation relation for continuous Markov processes.

On the other hand, things for the functional $\bar{W}(\tau)$ are much easier. The PDFs of $\bar{W}(\tau)$ always yield deviations from the Gaussian, but weaker than those observed for $W(\tau)$. The ES fluctuation relation is always fairly satisfied in all nonequilibrium cases at all times τ. The verification of both fluctuation relations is meaningless in the equilibrium cases ($a_2 = 0$) because $as_\tau \equiv 0$.

C. Difference between the fluctuations of $W(\tau)$ and of $\bar{W}(\tau)$

As already noted, the two action functionals defined in formula (23) differ for a *boundary term*. In principle, one

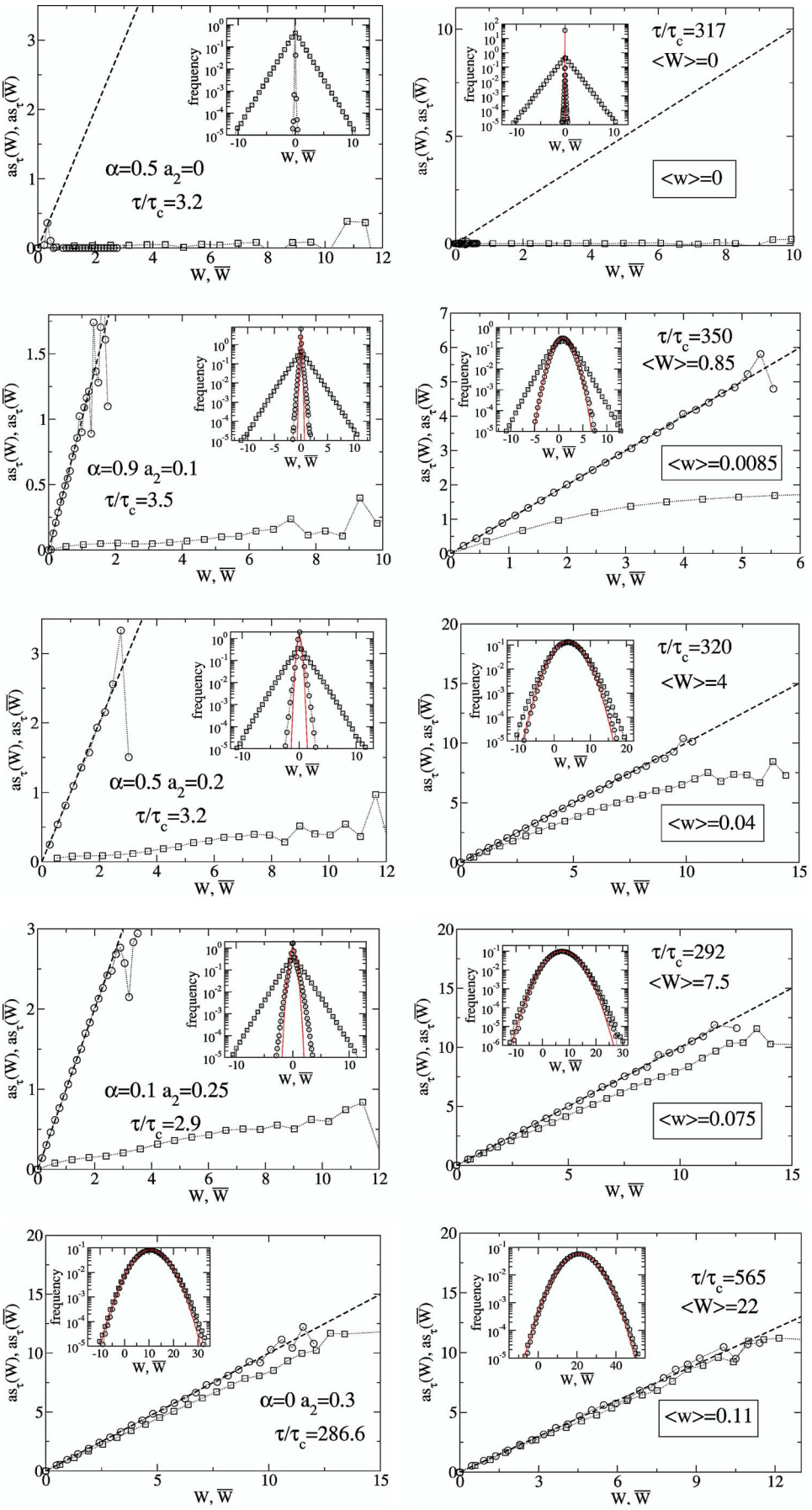

FIG. 2. (Color online) Verification of the fluctuation relations for $W(\tau)$ (squares) and $\bar{W}(\tau)$ (circles). Each line is composed of two graphs and shows the results for a particular choice of α and a_2: the left graph is at small times and the right graph at large times. In each frame, the inset contains the PDFs of W and $\bar{W}$, while the main plot shows $as_\tau(W)$ vs W as well as $as_\tau(\bar{W})$ vs $\bar{W}$. The red (solid) line in the insets is a Gaussian fit for the PDF of $\bar{W}$. The times τ are rescaled with the tracer mean free time τ_c (which varies with the parameters). For each choice of parameters, inside the right graph, we show the value of $\langle W(\tau)\rangle$ and of $\langle w\rangle \equiv \langle W(\tau)\rangle/\tau \equiv \langle \bar{W}(\tau)\rangle/\tau \equiv \lim_{\tau\to\infty} W(\tau)/\tau \equiv \lim_{\tau\to\infty} \bar{W}(\tau)/\tau$, which marks the distance from equilibrium. The dashed line has slope 1.

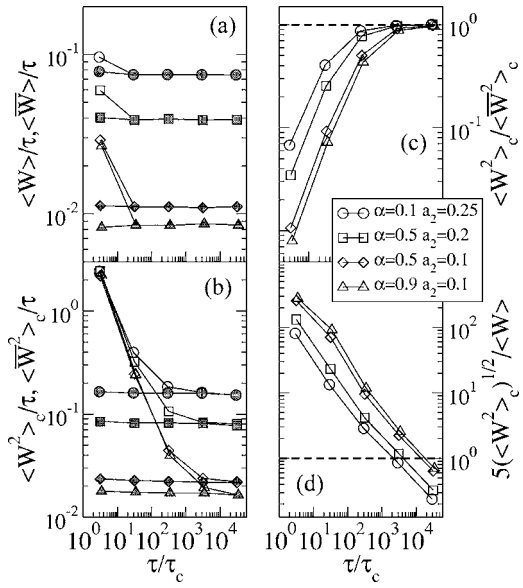

FIG. 3. Cumulants of the fluctuations of $W(\tau)$ (empty symbols) and $\bar{W}(\tau)$ (solid symbols). (a) Average values of $W(\tau)$ and $\bar{W}(\tau)$ as a function of τ and for different choices of the parameters α and a_2. (b) Second cumulants of $W(\tau)$ and $\bar{W}(\tau)$ as a function of τ. (c) Ratio between the second cumulant of $\bar{W}(\tau)$ and that of $W(\tau)$ as a function of τ. (d) Ratio between $5\sqrt{\langle W(\tau)^2\rangle_c}$ and $\langle W(\tau)\rangle$. When this ratio is much smaller than 1, the probability of observing negative events in the fluctuations of $W(\tau)$ becomes extremely low. All the times τ are rescaled by the tracer mean free time.

should expect that it is not possible to distinguish between the large deviations (i.e., the leading factor of the PDF at large times) of $W(\tau)$ and $\bar{W}(\tau)$. Anyway, there are no arguments to predict the threshold time above which the two functionals (i.e., most of their fluctuations) become indistinguishable from the point of view of large deviations [19,20]. Moreover, to our knowledge, it is not proved that the large deviation functions of W and $\bar{W}$ coincide. In this section, we first discuss numerical observations: they concern, generically, "deviations," i.e., fluctuations at finite time and finite values of the variables. Finally, we also argue about the asymptotic behavior of the PDFs of W and $\bar{W}$. As already stated, in numerical experiments, averages have been always obtained using many independent segments of length τ from a very long trajectory. This amounts to sampling the stationary velocity PDF of the tracer.

In Fig. 3, we have summed up the results of numerical simulations with different values of α, a_2, and τ. The averages $\langle W(\tau)\rangle$ and $\langle \bar{W}(\tau)\rangle$ converge to the same value in a time smaller than 100 average collision times [Fig. 3(a)]. The analysis of fluctuations [Figs. 3(b) and 3(c)], by means of the measure of their variance, instead indicates that the convergence is much more slower. Remarkably, the convergence is slower when the system is closer to equilibrium. We also tried to answer to the question of whether or not it is possible to verify the fluctuation relation FR_W at finite times in the regime (large τ) where the two functionals have negligible differences. The main obstacle to the verification of a fluctuation relation is the lack of negative events at large values of τ. The probability of finding a negative event is equivalent to the probability of finding a negative deviation from the mean of the order of the mean itself. We have seen that when the PDF of $W(\tau)$ seems to converge to its asymptotic scaling form, its tails are not far from those of a Gaussian and the bulk (i.e., its "small deviation" range) is clearly Gaussian. This means that there is a very sensitive decay of probability in the range of a finite number of standard deviations from the mean. From a numerical point of view, it is very unlikely to observe values of $W(\tau)$ below the value $\langle W(\tau)\rangle - 5\sqrt{\langle W^2(\tau)\rangle_c}$, where $\langle W^m(\tau)\rangle_c$ is the mth cumulant of $W(\tau)$ or, equivalently, that it is very unlikely to observe negative events if $5\sqrt{\langle W^2(\tau)\rangle_c} \ll \langle W(\tau)\rangle$. Figure 3(d) shows the ratio between $5\sqrt{\langle W^2(\tau)\rangle_c}$ and $\langle W(\tau)\rangle$. The conclusion of this analysis is that when τ is large enough to guarantee, at least at the level of the second cumulant, the convergence of the PDF of W (or its convergence to the PDF of $\bar{W}$), the probability of observing negative events is so small that huge statistics is required, in order to make reliable measurement of the fluctuation relation.

We now discuss one possible reason for such a slow convergence of the PDF of the fluctuations of $W(\tau)$. We will call it the "boundary term catastrophe." As a matter of fact, it seems that $W(\tau)$, even at very large values of τ, more evidently in the close-to-equilibrium cases, *remembers* its own small time fluctuations. This is clearly seen in the top four panels of Fig. 2. The tails of $W(\tau)$ at large τ are almost identical to those at small τ. What is happening? If one looks closely at expression (17), which is summed over many collisions to give $W(t)$, one discovers that

$$W(t) = \frac{3-\alpha}{1+\alpha}\frac{|\mathbf{v}_1|^2 - |\mathbf{v}_{n(t)}|^2}{2T} + \sum \log \frac{1+a_2\cdots}{1+a_2\cdots}, \qquad (41)$$

where we have used a shortened notation to identify the "nonequilibrium" part, which is the sum over all the collisions in the time τ of the logarithms of ratios between the Sonine contributions. The sum of the energy differences reduces to a difference between the first and last terms, which we can call again a "boundary term." It is easy to realize that the PDF of this term alone, being the PDF of a difference of energies, has exponential tails (in granular gases they can be even slower). This is the dominant term in the fluctuations of $W(\tau)$ at small τ, and it can dominate the fluctuations of $W(\tau)$ even at very large τ, depending on the amplitude of the fluctuations of the "Sonine" term. The Sonine term is small near equilibrium and increases as the system gets farther from equilibrium. This explains why the memory is stronger (i.e., convergence is lower) as the system is closer to equilibrium.

The situation dramatically changes when looking at the second functional, $\bar{W}(\tau)$. The boundary term discussed above almost perfectly annihilates with the boundary term appearing in the definition of $\bar{W}(t)$. Following the numerical observation that the PDF P_* of the velocity of the tracer is almost Gaussian with temperature $T_* \approx T' \equiv (1+\alpha)/(3-\alpha)T$, in fact, we see that

$$\log \frac{P_*(\mathbf{v}_1)}{P_*(\mathbf{v}_{n(t)})} \approx \frac{-|\mathbf{v}_1|^2+|\mathbf{v}_{n(t)}|^2}{2T_*} \approx \frac{3-\alpha}{1+\alpha}\frac{-|\mathbf{v}_1|^2+|\mathbf{v}_{n(t)}|^2}{2T}. \tag{42}$$

The error in this approximation is of the same order of one of the Sonine terms appearing in the sum (41) and is therefore subleading at large times. This crucial observation explains the absence of exponential tails in the PDF of $\bar{W}(t)$.

It should be stressed that this "boundary-term catastrophe" has relevant consequences not only in the realm of numerical simulations, but also from the point of view of large deviation theory. We suspect that, even with a computer of infinite power, i.e., with the ability of measuring with infinite quality the PDF of $W(\tau)$ at any time τ, the results of a large deviation analysis would yield similar results: the exponential tails related to the PDF of the $v_1^2-v_n^2$ are never forgotten. This is the consequence of the following simple observation: following the definition of "large deviations rate" of a PDF f_t that depends on a parameter t, we can also calculate the large deviations rate of a PDF F that does *not* depend on that parameter. We recall the definition

$$\pi(w) = \lim_{t\to\infty} \frac{1}{t} \log f_t(tw). \tag{43}$$

It can be immediately seen that such a definition gives a *finite* result if applied to a PDF F with exponential tails, even if it does not depend on t. This is equivalent to state that exponential tails always contribute to large deviations. The apparent loss of memory that can be observed in the strong nonequilibrium cases of Fig, 2 is only due to the limited range available in the measure of the PDF; these tails, in fact, get farther and farther as time increases. Moreover, we recall that such exponential tails are associated to the distribution of energy fluctuations and are always present in a system with a finite number of particles, not only in the one-particle case. They disappear only in the thermodynamic limit or in the presence of physical boundaries. We conclude this discussion mentioning that the boundary term catastrophe is responsible for the failure of GC fluctuation relation in other systems [19–22].

V. CONCLUSIONS

In conclusion, we have studied the dynamics of a tracer particle in a driven granular gas. The tracer performs a sequence of collisions changing its velocity, thus, performing a Markov process with transition rates that can be obtained from the linear Boltzmann equation. We have given a general expression for these rates and have also calculated them for a number of possible interesting cases. There is a major discrimination between the Gaussian and non-Gaussian cases, depending on the velocity distribution of the gas particles. In the Gaussian case, the tracer is at equilibrium, even if the collisions are dissipative and energy equipartition is not satisfied. In the non-Gaussian case, the tracer reaches a statistically stationary nonequilibrium state: in this state, a dissipative flow can be measured in the form of an action functional that has been defined by Lebowitz and Spohn [9]. The average of this flow well describes the distance from equilibrium. Moreover, the rate of variation of the entropy of the tracer can be split up into two contributions, one always positive and the second given by the average of this dissipative flux. Following the Lebowitz and Spohn "recipe," we have tried to verify the Gallavotti-Cohen fluctuation relation for the action functional, realizing that this verification is not accessible. At the same time, we have perfectly verified a second fluctuation relation, for a slightly different functional, which we have called the Evans-Searles fluctuation relation because of a formal analogy with it. We have discussed the possibility that a nonextensive term (in time) in the definition of the Lebowitz-Spohn functional can spoil the applicability of the large deviation principle. In our numerical simulations, we have also very well verified the correctness of the formula for the transition rates, showing a way to optimize their measure in real experiments. A key point of our work is, in fact, that such Lagrangian approach in granular gas theory should be applied to experiments on dilute granular matter, in order to directly test the limits of the different fluctuation relations. Future work will be directed to the study of transients and nonhomogeneous situations. The Evans-Searles fluctuation relation is expected to hold also in nonstationary regimes, such as the transient relaxation of a packet of noninteracting tracer granular particles prepared in some nontypical initial state. Nonhomogeneous situations, such as a boundary-driven granular gas but also ordinary thermostatted molecular gases driven out of equilibrium by a nonconservative force (such as a shear), are characterized by the presence of spatially directed fluxes. It will be interesting to study the "action functional" defined in this work and compare it to other measures of transport.

ACKNOWLEDGMENTS

The authors acknowledge A. Barrat for several fruitful discussions. A.P. warmly thanks L. Rondoni for discussions and acknowledges the Marie Curie Grant No. MEIF-CT-2003-500944.

APPENDIX: DERIVATION FROM THE LINEAR BOLTZMANN EQUATION

We first discuss, in detail, what happens in a collision and then give a rigorous derivation of the master equation. The collision rule for inelastic hard spheres reads

$$\mathbf{v}_1' = \mathbf{v}_1 - \frac{1+\alpha}{2}(\mathbf{v}_{12}\cdot\hat{\boldsymbol{\sigma}})\hat{\boldsymbol{\sigma}}, \tag{A1}$$

where $\hat{\boldsymbol{\sigma}}$ is the direction joining the centers of the two colliding particles. There are some consequences of the collision rules that have to be remarked. For simplicity, we assume to be in dimension $d=2$.

(i) $\Delta\mathbf{v}_1=\mathbf{v}_1'-\mathbf{v}_1$ is parallel to $\hat{\boldsymbol{\sigma}}$, i.e., $\theta=\arctan\Delta v_{1y}/\Delta v_{1x}$, where $\hat{\sigma}_x=\cos\theta$ and $\hat{\sigma}_y=\sin\theta$. This is equivalent to recognize that the velocity $\mathbf{v}_1$ changes only in the direction $\hat{\boldsymbol{\sigma}}$. The fact that $\mathbf{v}_{12\sigma}$ must be negative determines, completely, the angle θ, i.e., the unitary vector $\hat{\boldsymbol{\sigma}}$. From here on, we call $\Delta v_1 \equiv \Delta v_{1\sigma} \equiv \Delta\mathbf{v}_1\cdot\hat{\boldsymbol{\sigma}}$.

(ii) $v_{2\sigma} \equiv \mathbf{v}_2 \cdot \hat{\boldsymbol{\sigma}} = [2/(1+\alpha)]\Delta v_1 + v_{1\sigma} = [2/(1+\alpha)]v'_{1\sigma} - [(1-\alpha)/(1+\alpha)]v_{1\sigma}$.

(iii) From the previous two remarks, it is clear that Δv_1 determines univocally $\hat{\boldsymbol{\sigma}}$ and $v_{2\sigma}$. The component of $\mathbf{v}_2$ that is not determined by Δv_1 is the one orthogonal to $\hat{\boldsymbol{\sigma}}$. We call $\hat{\boldsymbol{\tau}}$ the direction perpendicular to $\hat{\boldsymbol{\sigma}}$, i.e., the vector of component $(-\sin\theta, \cos\theta)$. We define $v_{2\tau} = \mathbf{v}_2 \cdot \hat{\boldsymbol{\tau}}$.

From the above discussion, it is easy to understand that the transition probability for particle 1 to change velocity during a collision, going from $\mathbf{v}_1$ to $\mathbf{v}'_1$ must be

$$K(\mathbf{v}_1 \to \mathbf{v}'_1) = C(\mathbf{v}_1, \mathbf{v}'_1) \int \mathrm{d}v_{2\tau} P(\mathbf{v}_2) \tag{A2}$$

$$\mathbf{v}_2 = v_{2\sigma}\hat{\boldsymbol{\sigma}} + v_{2\tau}\hat{\boldsymbol{\tau}} \tag{A3}$$

$$\hat{\boldsymbol{\sigma}} = (\cos\theta, \sin\theta) \tag{A4}$$

$$\hat{\boldsymbol{\tau}} = (-\sin\theta, \cos\theta) \tag{A5}$$

$$\theta = \arctan\frac{\Delta v_{1y}}{\Delta v_{1x}} \tag{A6}$$

$$\hat{\boldsymbol{\sigma}} \| \mathbf{v}'_1 - \mathbf{v}_1 \tag{A7}$$

$$v_{2\sigma} = \frac{2}{1+\alpha}\Delta v_1 + v_{1\sigma}, \tag{A8}$$

where $P(\mathbf{v})$ is the one-particle probability density function for the velocity in the bulk gas. The constant of proportionality C must be of dimensions $1/\mathit{length}$ so that K has dimensions $1/(\mathit{velocity}^d \mathit{time})$, which is expected because K is a rate of change of the velocity PDF (in d dimensions).

Now, we want to obtain the complete result, that is rigorously transform the usual linear γ-Boltzmann equation for inelastic models in a master equation for a single-particle Markov chain, i.e., as

$$\frac{\mathrm{d}P_*(\mathbf{v},t)}{\mathrm{d}t} = \int \mathrm{d}\mathbf{v}_1 P_*(\mathbf{v}_1) K(\mathbf{v}_1 \to \mathbf{v}) - \int \mathrm{d}\mathbf{v}_1 P_*(\mathbf{v}) K(\mathbf{v} \to \mathbf{v}_1), \tag{A9}$$

with $P_*(v)$ the velocity PDF of the test particle.

From this definition [and from the usual linear Boltzmann equation for models containing a term $|\mathbf{v}_{12}\cdot\hat{\boldsymbol{\omega}}|^\gamma$, Eq. (3)], it follows that

$$K(\mathbf{v}_1 \to \mathbf{v}'_1) = \frac{v_0^{1-\gamma}}{l_0} \int \mathrm{d}\mathbf{v}_2 \int \mathrm{d}\hat{\boldsymbol{\omega}} \Theta(\mathbf{v}_{12}\cdot\hat{\boldsymbol{\omega}}) \times |\mathbf{v}_{12}\cdot\hat{\boldsymbol{\omega}}|^\gamma P(\mathbf{v}_2) \delta\left\{\mathbf{v}'_1 - \mathbf{v}_1 + \frac{1+\alpha}{2}[\mathbf{v}_{12}\cdot\hat{\boldsymbol{\omega}}]\hat{\boldsymbol{\omega}}\right\}, \tag{A10}$$

where $P(v)$ is the velocity PDF of the bulk gas. Using that for a generic d-dimensional vector $\mathbf{r} = r\hat{\mathbf{r}}$, one has $\delta(\mathbf{r}-\mathbf{r}_0) = (1/r_0^{d-1})\delta(r-r_0)\delta(\hat{\mathbf{r}}-\hat{\mathbf{r}}_0)$, the previous expression can be rewritten as

$$K(\mathbf{v}_1 \to \mathbf{v}'_1) = \frac{v_0^{1-\gamma}}{l_0} \int \mathrm{d}\mathbf{v}_2 \int \mathrm{d}\hat{\boldsymbol{\omega}} \Theta(\mathbf{v}_{12}\cdot\hat{\boldsymbol{\omega}}) \frac{|\mathbf{v}_{12}\cdot\hat{\boldsymbol{\omega}}|^\gamma}{\Delta v^{d-1}} \times P(\mathbf{v}_2)\delta(\hat{\boldsymbol{\sigma}}+\hat{\boldsymbol{\omega}})\delta\left(\Delta v + \frac{1+\alpha}{2}|\mathbf{v}_{12}\cdot\hat{\boldsymbol{\omega}}|\right), \tag{A11}$$

where Δv and $\hat{\boldsymbol{\sigma}}$ are defined by $\mathbf{v}'_1 - \mathbf{v}_1 = \Delta v \hat{\boldsymbol{\sigma}}$. Then, performing the angular integration over $\hat{\boldsymbol{\omega}}$, one obtains

$$K(\mathbf{v}_1 \to \mathbf{v}'_1) = \frac{v_0^{1-\gamma}}{l_0} \int \mathrm{d}\mathbf{v}_2 \Theta(\mathbf{v}_{12}\cdot\hat{\boldsymbol{\sigma}}) \frac{|\mathbf{v}_{12}\cdot\hat{\boldsymbol{\sigma}}|^\gamma}{\Delta v^{d-1}} \times P(\mathbf{v}_2)\delta\left(\Delta v + \frac{1+\alpha}{2}|\mathbf{v}_{12}\cdot\hat{\boldsymbol{\sigma}}|\right). \tag{A12}$$

Denoting by $v_{2\sigma}$ the component of $\mathbf{v}_2$ parallel to $\hat{\boldsymbol{\sigma}}$, and by $\mathbf{v}_{2\tau}$ the $(d-1)$-dimensional vector in the hyperplane perpendicular to $\hat{\boldsymbol{\sigma}}$, Eq. (A12) is rewritten as

$$K(\mathbf{v}_1 \to \mathbf{v}'_1) = \frac{v_0^{1-\gamma}}{l_0} \int \mathrm{d}v_{2\sigma}\mathrm{d}\mathbf{v}_{2\tau} \Theta(\mathbf{v}_{12}\cdot\hat{\boldsymbol{\sigma}}) \frac{|\mathbf{v}_{12}\cdot\hat{\boldsymbol{\sigma}}|^\gamma}{\Delta v^{d-1}} \times P(v_{2\sigma}, \mathbf{v}_{2\tau})\delta\left(\Delta v + \frac{1+\alpha}{2}|\mathbf{v}_{12}\cdot\hat{\boldsymbol{\sigma}}|\right). \tag{A13}$$

Finally, integrating over $\mathrm{d}v_{2\sigma}$, Eq. (5) is easily recovered.

[1] *Granular Gases*, edited by T. Pöschel and S. Luding, Lecture Notes in Physics Vol. 564 (Springer, New York, 2001).

[2] A. Barrat, E. Trizac, and M. H. Ernst, J. Phys.: Condens. Matter **17**, S2429 (2005).

[3] J. J. Brey, J. W. Dufty, C. S. Kim, and A. Santos, Phys. Rev. E **58**, 4638 (1998).

[4] A. Prevost, D. A. Egolf, and J. S. Urbach, Phys. Rev. Lett. **89**, 084301 (2002).

[5] G. Gallavotti and E. G. D. Cohen, Phys. Rev. Lett. **74**, 2694 (1995).

[6] K. Feitosa and N. Menon, Phys. Rev. Lett. **92**, 164301 (2004).

[7] S. Aumaître, S. Fauve, S. McNamara, and P. Poggi, Eur. Phys. J. B **19**, 449 (2001).

[8] P. Visco, A. Puglisi, A. Barrat, E. Trizac, and F. van Wijland, Europhys. Lett. **72**, 55 (2005); A. Puglisi, P. Visco, A. Barrat, E. Trizac, and F. van Wijland, Phys. Rev. Lett. **95**, 110202 (2005).

[9] J. L. Lebowitz and H. Spohn, J. Stat. Phys. **95**, 333 (1999).

[10] P. A. Martin and J. Piasecki, Europhys. Lett. **46**, 613 (1999).

[11] J. J. Brey, M. J. Ruiz-Montero, R. Garcia-Rojo, and J. W.

Dufty, Phys. Rev. E **60**, 7174 (1999); J. J. Brey, J. W. Dufty, and A. Santos, J. Stat. Phys. **97**, 281 (1999); A. Santos and J. W. Dufty, Phys. Rev. Lett. **86**, 4823 (2001); A. Santos and J. W. Dufty, Phys. Rev. E **64**, 051305 (2001).

[12] D. J. Evans and D. J. Searles, Phys. Rev. E **50**, 1645 (1994).

[13] D. J. Evans and D. J. Searles, Adv. Phys. **51**, 1529 (2002).

[14] D. R. M. Williams and F. C. MacKintosh, Phys. Rev. E **54**, R9 (1996); A. Puglisi, V. Loreto, U. M. B. Marconi, A. Petri, and A. Vulpiani, Phys. Rev. Lett. **81**, 3848 (1998); T. P. C. van Noije and M. Ernst, Granular Matter **1**, 57 (1998); G. Peng and T. Ohta, Phys. Rev. E **58**, 4737 (1998); T. P. C. van Noije, M. H. Ernst, E. Trizac, and I. Pagonabarraga, *ibid.* **59**, 4326 (1999); C. Henrique, G. Batrouni, and D. Bideau, *ibid.* **63**, 011304 (2000); S. J. Moon, M. D. Shattuck, and J. B. Swift, *ibid.* **64**, 031303 (2001); I. Pagonabarraga, E. Trizac, T. P. C. van Noije, and M. H. Ernst, *ibid.* **65**, 011303 (2002).

[15] Sonine polynomials are often used to construct solutions to the Boltzmann equation. They are exact eigenfunctions of the linearized Boltzmann collision operator for elastic Maxwell molecules, i.e., particles interacting with repulsive r^{-4} potentials. They are discussed in great detail in S. Chapman and T. G. Cowling, *The Mathematical Theory of Non-Uniform Gases* (Cambridge University Press, Cambridge, England, 1970).

[16] C. Maes, J. Stat. Phys. **95**, 367 (1999).

[17] J. Kurchan, J. Phys. A **31**, 3719 (1998).

[18] G. A. Bird, *Molecular Gas Dynamics and the Direct Simulation of Gas Flows* (Clarendon, Oxford, 1994); J. M. Montanero and A. Santos, Granular Matter **2**, 53 (2000).

[19] D. J. Evans, D. J. Searles, and L. Rondoni, Phys. Rev. E **71**, 056120 (2005).

[20] F. Bonetto, G. Gallavotti, A. Giuliani, and F. Zamponi, e-print cond-mat/0507672.

[21] J. Farago, J. Stat. Phys. **107**, 781 (2002).

[22] R. van Zon and E. G. D. Cohen, Phys. Rev. Lett. **91**, 110601 (2003).